Journal of Electrochemical Science and Technology
Vol. 3, No. 2, 2012, 63-67
http://dx.doi.org/10.5229/JECST.2012.3.2.63

Journal of Electrochemical Science and Technology

Electrochemical Properties and Thermal Stability of $LiNi_{0.8}Co_{0.15}Al_{0.05}O_2$-$LiFePO_4$ Mixed Cathode Materials for Lithium Secondary Batteries

Hyun-Ju Kim, Bong-Soo Jin, Chil-Hoon Doh and Hyun-Soo Kim†
Battery Research Center, Korea Electrotechnology Research Institute, Changwon 641-120, Korea

ABSTRACT :

We prepared various $LiNi_{0.8}Co_{0.15}Al_{0.05}O_2$-$LiFePO_4$ mixed-cathode electrodes by changing the content of $LiNi_{0.8}Co_{0.15}Al_{0.05}O_2$ and $LiFePO_4$ used, and we analyzed the electrochemical characteristics of the cathodes. We found that the reversible specific capacity of the cathodes increased and that the capacity retention ratios of the cathodes decreased during cycling as the content of $LiNi_{0.8}Co_{0.15}Al_{0.05}O_2$ increased. Conversely, we found that although the reversible specific capacity of the cathodes decreased because of the material composition, the cycle property of the cathodes increased when the $LiFePO_4$ content increased. We analyzed the thermal stability of the $LiNi_{0.8}Co_{0.15}Al_{0.05}O_2$-$LiFePO_4$ mixed-material cathodes by differential scanning calorimetry and found that it increased as the $LiFePO_4$ content increased.

Keywords: $LiNi_{0.8}Co_{0.15}Al_{0.05}O_2$, $LiFePO_4$, Thermal stability, Mixed-cathode, Cycle property

Received May 8, 2012 : Accepted June 22, 2012

1. Introduction

Numerous cathode materials have been developed for lithium-ion batteries to improve battery performance. The most widely used commercial cathode material for lithium-ion batteries is $LiCoO_2$ because it is easy to produce and is stable during electrochemical cycling. Much current research is focused on replacing $LiCoO_2$ with safer alternatives by developing nontoxic, higher-capacity, lower-cost cathode materials. $LiNiO_2$ is superior to $LiCoO_2$ because of its lower cost and higher specific capacity[1]; however, its thermal instability and poor cycling reversibility prevent its practical use as a cathode material. $LiNi_{0.8}Co_{0.15}Al_{0.05}O_2$ is a promising cathode material because of its improved stability and electrochemical performance from substitution of Co and Al for Ni in $LiNiO_2$.[2-5] Since the ionic radii of Co^{3+} and Al^{3+} are smaller than the ionic radius of Ni^{3+}, substituting these ions for Ni^{3+} results in shrinkage of the *a*-axis, which is believed to help stabilize the layered structure.[6] Although the high capacity of this material is very advantageous, a critical drawback is its structural instability in a highly oxidized state, as was previously confirmed by differential scanning calorimetry (DSC).[7]

Lithium iron phosphate ($LiFePO_4$), on the other hand, is a promising cathode material for use in lithium rechargeable batteries. It has many advantages over conventional cathode materials, such as $LiCoO_2$, $LiNiO_2$, and $LiMn_2O_4$: It is environmentally benign, inexpensive, and thermally stable when fully charged.[8,9] Moreover, $LiFePO_4$ has excellent thermal safety because of the strong covalent bond properties of PO_4, making it highly suitable for manufacturing electric vehicle (EV) batteries.[10,11]

Therefore, It can obtain both high capacity and safety of mixed electrode from $LiNi_{0.8}Co_{0.15}Al_{0.05}O_2$ and $LiFePO_4$, respectively. In this paper we have confirmed electrochemical performance and behavior of

†Corresponding author. Tel.: +82-55-280-1699
E-mail address: hskim@keri.re.kr

thermal stability of $LiNi_{0.8}Co_{0.15}Al_{0.05}O_2$-$LiFePO_4$ mixed electrode by blending ratio.

2. Experimental

The $LiNi_{0.8}Co_{0.15}Al_{0.05}O_2$-$LiFePO_4$ mixed-material cathodes were prepared and their electrochemical properties were measured at a high cut-off voltage. First, the materials were prepared by blending $LiNi_{0.8}Co_{0.15}Al_{0.05}O_2$ (ECOPRO) and $LiFePO_4$ (Dea-jung E.M.) in 100:0, 75:25, 50:50, 25:75, and 0:100 wt% ratios. The respective electrode compositions and notations are listed in Table 1.

X-ray diffraction (XRD) analysis was performed using an X-pert PW3830 (Philips Co.) to observe the crystal structure and any impurities in the synthesized active materials. The Cu Ká line was used under 40 kV and 30 mA conditions, with a 0.04°/s scan speed and a 10-70° (2θ) scan range. In addition, field emission scanning electron microscopy (FE-SEM, S-4800, Hitachi Co.) analysis was conducted to measure the particle size and surface morphology of the materials. Before the XRD analysis, Os was coated onto the surface of the specimens to enhance their electrical conductivity.

The active materials ($LiNi_{0.8}Co_{0.15}Al_{0.05}O_2$-$LiFePO_4$), a conducting agent (Super-P conductive carbon black), and a binder (polyvinylidene fluoride (PVDF)) were dissolved in *N*-methyl-2-pyrrolidone (NMP) in a 70:20:10 wt% ratio to obtain a slurry so that the electrochemical properties of the synthesized active materials could be measured. The slurry was then coated onto aluminum foil and dried for 12 hours at 100°C. The cathode electrodes were then prepared by pressing the coated aluminum foil with a hot-roll press at 110°C. A lithium anode, a separator (Celguard 3501), and a cathode electrode were then laminated for assembly into coin cells (CR2032 type). Ethylene carbonate (EC) and dimethyl ethyl carbonate (DEC) were mixed in a 1:1 volumetric ratio, and dissolved $LiPF_6$ was used as the electrolyte.

Table 1. Compositions and notations of $LiNi_{0.8}Co_{0.15}Al_{0.05}O_2$-$LiFePO_4$ mixed cathode materials.

Electrode composition (wt%)	Notation
NCA:LFP = 100:0	100 wt% NCA
NCA:LFP = 75:25	75 wt% NCA
NCA:LFP = 50:50	50 wt% NCA
NCA:LFP = 25:75	25 wt% NCA
NCA:LFP = 0:100	100 wt% LFP

The electrochemical properties of the synthesized $LiNi_{0.8}Co_{0.15}Al_{0.05}O_2$-$LiFePO_4$ cathode materials were measured using a battery cycler (TOCAT-3100, TOYO System). The materials were charged and discharged over a 2.0-4.3 V range by the constant-current, constant-voltage (CCCV) charging method. Rate capability was evaluated at current rates 0.1, 0.2, 0.5, 1.0, 3.0, 5.0, 10, and 20 C. The cycling performance of the synthesized $LiNi_{0.8}Co_{0.15}Al_{0.05}O_2$-$LiFePO_4$ materials were also tested at 0.5 C. The electrodes were fully charged at 4.3 V, and DSC (Q1000, TA instruments, USA) was performed to measure the thermal stability of the $LiNi_{0.8}Co_{0.15}Al_{0.05}O_2$-$LiFePO_4$ mixed cathode electrodes. Electrochemical impedance spectroscopy (EIS) was measured for the discharged cells by using an IM6 system (ZAHNER, Germany). The frequency range was measured in the 1 Hz-1 MHz range, and the amplitude was measured in increments of 10 mV.

3. Results and Discussion

Fig. 1 shows the XRD spectra for the pure and mixed-material cathodes. The spectra in Figs. 1(a) and (e) show peaks consistent with the olivine structure of 100 wt% LFP and the layered structure of 100 wt% NCA. The spectra in Figs. 1(b), (c), and (d) show peaks consistent with coexistent olivine and layered structures in the mixed-material cathodes.

Fig. 2 is an FE-SEM image showing the relative shapes and sizes of $LiNi_{0.8}Co_{0.15}Al_{0.05}O_2$ (Fig. 2(a)) and $LiFePO_4$ (Fig. 2(b)) particles. The 100 wt% LFP particles are less than 500 nm and are a mixture of

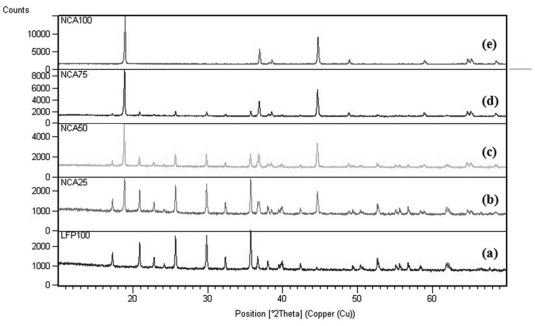

Fig. 1. XRD patterns for $LiNi_{0.8}Co_{0.15}Al_{0.05}O_2$-$LiFePO_4$ mixed cathode materials: (a) 100 wt% LFP, (b) 25 wt% NCA, (c) 50 wt% NCA, (d) 75 wt% NCA, (e) 100 wt% NCA.

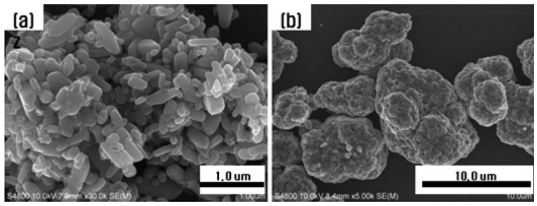

Fig. 2. FE-SEM images of $LiNi_{0.8}Co_{0.15}Al_{0.05}O_2$ and $LiFePO_4$ cathode materials: (a) 100 wt% LFP, (b) 100 wt% NCA.

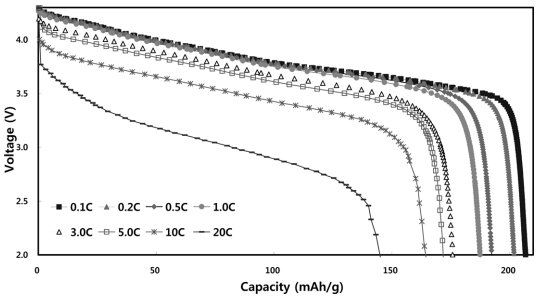

Fig. 3. Rate capability of 100 wt% NCA cathode material.

globular and bar shapes. The 100 wt% NCA particles, on the other hand, are less than 7 μm and are only globular.

Figs 3-6 show the charge and discharge curves for the secondary Li batteries corresponding to the mixed-material cathodes produced with different compositions of $LiNi_{0.8}Co_{0.15}Al_{0.05}O_2$ and $LiFePO_4$. Charging and discharging proceeded up to the 4.3–2.0 V range.

Fig. 3 shows the discharge curve corresponding to the discharge current of the battery using only 100 wt% NCA. The discharge capacity decreases gradually from its initial value of approximately 206.8 $mAhg^{-1}$ to 192.3, 187.5, 175.8, and 172 $mAhg^{-1}$, corresponding to 0.5, 1.0, 3.0, and 5.0 C increases in the current ratio.

This represents a decrease in voltage, corresponding to increased inner resistance because the Li ions cannot move in response to increased discharge current. However, even at the 20 C rate, this battery has an excellent 145 $mAhg^{-1}$ rate and a 70% capacity retention ratio compared with its initial discharge capacity, as shown in Fig. 3.

Fig. 4 is a graph showing the rate characteristics of the 100 wt% LFP cathode. The discharge capacity decreases gradually from its initial value of approximately 157.4 $mAhg^{-1}$ to 153.9, 152, 142.9, and 136.1 $mAhg^{-1}$, corresponding to 0.5, 1.0, 3.0, and 5.0 C

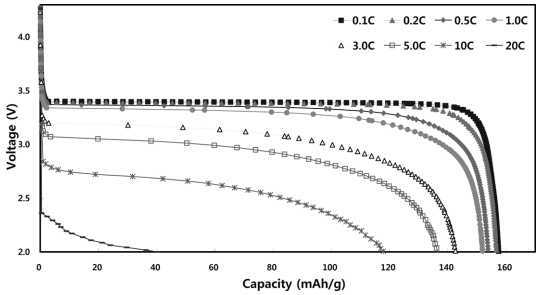

Fig. 4. Rate capability for 100 wt% LFP cathode material.

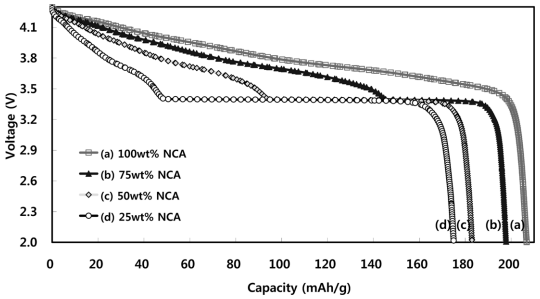

Fig. 5. Initial discharge curves for $LiNi_{0.8}Co_{0.15}Al_{0.05}O_2$-$LiFePO_4$ mixed cathode materials.

increases in the current ratio. Moreover, even at the 10 C rate exhibited a 116.9 $mAhg^{-1}$ rate characteristic and a 74.3% capacity retention ratio compared with its initial discharge capacity.

Fig. 5 shows the initial discharge capacity profiles of the mixed-cathode materials produced with different compositions of $LiNi_{0.8}Co_{0.15}Al_{0.05}O_2$ and $LiFePO_4$. As shown in the figure, the greater the NCA content in the mixed-material cathode composition, the greater the reversible specific capacity becomes, and it decreases as NCA content decreases. The discharge profiles for the mixed-material cathodes all show similar behavior. Further, the plateau area of the profile for $LiFePO_4$ shows stable positive power characteristics in the relatively low-voltage zone around 3.4 V.

Fig. 6 is a graph showing the rate characteristics of the 50 wt% NCA mixed cathode material battery. The discharging capacities decreased to 176.2, 170.9, 159.6, and 151.6 $mAhg^{-1}$ from an initial value of approximately 182.9 $mAhg^{-1}$, corresponding to 0.5, 1.0, 3.0, and 5.0 C increases in current ratio. The plateau area in the profile of $LiFePO_4$ is also in the relatively low-voltage zone around 3.4 V. Further, this exhibited a 139 $mAhg^{-1}$ rate characteristic, even at the

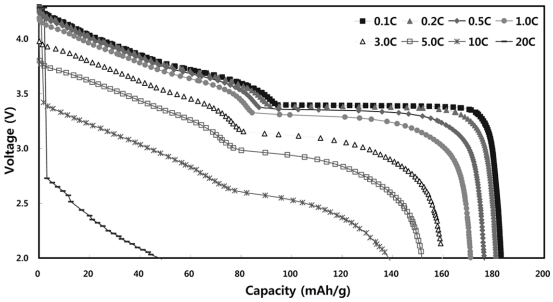

Fig. 6. Rate capability for 50 wt% NCA mixed cathode materials.

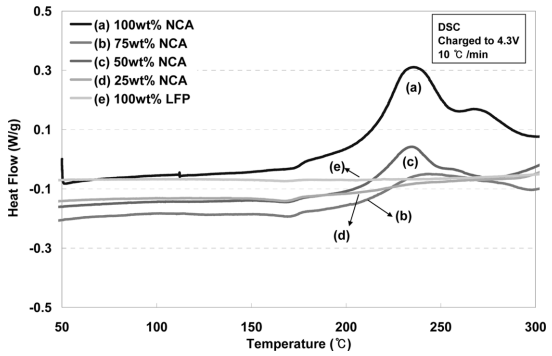

Fig. 7. DSC curves for $LiNi_{0.8}Co_{0.15}Al_{0.05}O_2$-$LiFePO_4$ mixed cathode materials.

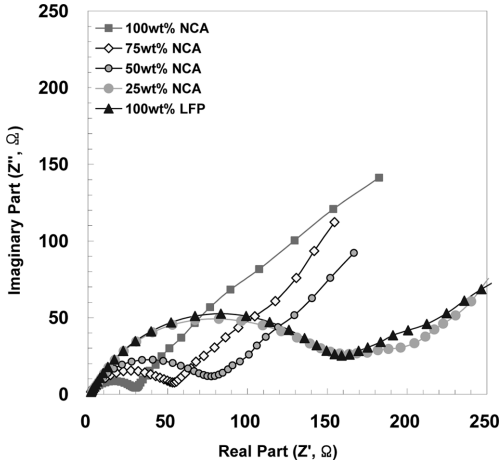

Fig. 8. EIS (Nyquist plots) for $LiNi_{0.8}Co_{0.15}Al_{0.05}O_2$-$LiFePO_4$ mixed cathode materials.

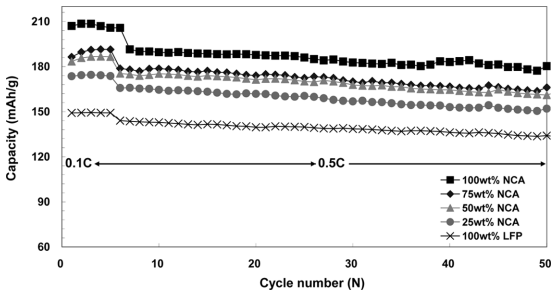

Fig. 9. Cycling performance of $LiNi_{0.8}Co_{0.15}Al_{0.05}O_2$-$LiFePO_4$ mixed cathode materials measured at 0.5 C current rate.

10 C rate, and its discharge profile shows similar behavior to those of the other mixed-material cathodes produced with different compositions of $LiNi_{0.8}Co_{0.15}Al_{0.05}O_2$ and $LiFePO_4$.

Fig. 7 is a graph showing the DSC results for the thermal-stability analysis of the mixed-cathode materials with different $LiNi_{0.8}Co_{0.15}Al_{0.05}O_2$ and $LiFePO_4$ contents. The results for the 100 wt% NCA material show an exothermic peak from approximately 208.5 to 233.56ºC with a 163.8 Jg^{-1} total heating value. The results for the 75 wt% and 50 wt% NCA materials, show total heating values of approximately 60.47 Jg^{-1} and 53.69 Jg^{-1}, respectively. As the $LiFePO_4$ content in the material increases, the total heating value decreases significantly. This might come from the structural and thermal stability of $LiFePO_4$.

We then measured the impedance characteristics of the mixed-material cathodes, fully discharged to 2.0 V. Fig. 8 shows the results of the impedance measurements for the mixed-material cathodes. The graph is composed of a semicircular area at high frequency and a curve at low frequency. The semicircle is probably due to resistance of the active material inside and on the interfaces of the electrodes, and the curve is due to diffused resistance of Li ions in the electrolyte. The higher the $LiNi_{0.8}Co_{0.15}Al_{0.05}O_2$ content, the lower the resistance becomes; and the charge-transfer resistance increases as the $LiFePO_4$ content increases. A sudden increase in resistance was observed for the 100 wt% LFP cathode.

Fig. 9 is a graph comparing the cycle performance of the mixed-material cathodes produced with different $LiNi_{0.8}Co_{0.15}Al_{0.05}O_2$ and $LiFePO_4$ contents. The cathodes were cycled 50 times at 0.5 C after cycling them 5 times at 0.1 C. The initial discharge capacity of the electrode was approximately 205.8 $mAhg^{-1}$, and that after charging and discharging 50 times was approximately 178.5 $mAhg^{-1}$, yielding an 86.7% capacity retention rate. Initially, the discharge capacity of the mixed-material cathodes increased as the

Table 2. Capacity retention ratios of $LiNi_{0.8}Co_{0.15}Al_{0.05}O_2$-$LiFePO_4$ mixed cathode materials after 50 cycles.

Samples	Initial discharge capacity ($mAhg^{-1}$)	Final discharge capacity ($mAhg^{-1}$)	Capacity retention ratio (%)
NCA 100	205.8	178.5	86.7
NCA 75	191.4	166.1	86.8
NCA 50	186.5	161.9	86.8
NCA 25	173.7	152.0	87.5
LFP 100	149.2	134.5	90.1

$LiNi_{0.8}Co_{0.15}Al_{0.05}O_2$ content increased, but after 50 cycles, it increased more in correlation with the increase in $LiFePO_4$ content. This might be the result of structural stability because of minimal movement in the ionic lattice during cycling, which is characteristic of the $LiFePO_4$ olivine structure.

As listed in Table 2, when ratio of $LiFePO_4$ increases, the capacity retention ratio increases from about 86.8 to 90.1% after 50 cycles.

4. Conclusions

We produced $LiNi_{0.8}Co_{0.15}Al_{0.05}O_2$-$LiFePO_4$ mixed-material cathodes by changing the content of the $LiNi_{0.8}Co_{0.15}Al_{0.05}O_2$ and $LiFePO_4$ used, and we analyzed the electrochemical characteristics of the cathodes. We found that the reversible specific capacity of the cathodes increased and that the capacity retention ratio of the cathodes decreased during cycling as the content of $LiNi_{0.8}Co_{0.15}Al_{0.05}O_2$ increased. Conversely, we found that although the reversible specific capacity of the cathodes decreased because of the material composition, the cycle property of the cathodes increased when the $LiFePO_4$ content increased. The excellent cycle property of the mixed-material cathodes might be the result of the stable olivine structure of $LiFePO_4$ because of minimal movement in the ionic lattice during cycling.

We analyzed the thermal stability of the $LiNi_{0.8}Co_{0.15}Al_{0.05}O_2$-$LiFePO_4$ mixed-material cathodes by DSC and found that it increased because of a decrease in the total heating value corresponding to an increase in the $LiFePO_4$ content.

Accordingly, peak points of both high capacity and stability can be achieved using $LiNi_{0.8}Co_{0.15}Al_{0.05}O_2$-$LiFePO_4$ mixed material cathode in this experiment.

References

1. T. Ohzuku, A. Ueda and M. Nagayama, J. Electrochem. Soc., **140**, 1862 (1993).
2. C. Delmas, I. Saadoune and A. Rougier, J. Power Sources, **44** 592 (1993).
3. M.R. Palacin, D. Larcher, A. Audemer, N. Sac-Epee, G.G. Amatucci and J.M. Tarascon, J. Electrochem. Soc., **144**, 4226 (1997).
4. E. Levi, M.D. Levi, G. Salitra, D. Aurbach, R. Oesten, U. Heider and L. Heider, Solid State Ionics, **126**, 97 (1999).
5. T. Ohzuku, A. Ueda and M. Kouguchi, J. Electrochem. Soc., **142**, 4033 (1995).
6. H. Cao, B. Xia, N. Xu and C. Zhang, J. Alloys Compd., **376**, 282 (2004).
7. T. Ohzuku, A. Ueda and M. Kouguchi, J. Electrochem. Soc., **142**, 4033 (1995).
8. A.S. Anderson and J.O. Thomas, J. Power Sources, 97-98, 498 (2001).
9. N. Ravet, M. Gauthier, K. Zaghib, J.B. Goodenough, A. Mauger, F. Gendron and C.M. Julien, J. Chem. Mater., **19**, 2595 (2007).
10. K. Zaghib, P. Charest, A. Guerfi, J. Shim, M. Perrier and K. Striebel, J. Power Sources, **146**, 380 (2005).
11. S. Beninati, L. Damen and M. Mastragostino, J. Power Sources, **180**, 875 (2008).